Atmospheric Research 213 (2018) 196–210

Contents lists available at ScienceDirect

Atmospheric Research

journal homepage: www.elsevier.com/locate/atmosres

Secular variation of rainfall regime in the central region of Argentina

Antonio C. de la Casa*, Gustavo G. Ovando, Guillermo J. Díaz

Facultad de Ciencias Agropecuarias, Universidad Nacional de Córdoba, Ing. Agr. Félix Aldo Marrone 746, Ciudad Universitaria 5000, Córdoba, Argentina

ARTICLE INFO

Keywords:
Rainfall regime
Climate change
Trend
Linear model
Periodic model

ABSTRACT

Apart from modifying the total amount of rain, another emerging impact of global warming on the rainfall regime could be an increase in the frequency and intensity of events, as well as their greater variability over time and space. The objectives of this work were to evaluate the long-term climatic variation of the precipitation regime in the central region of Argentina, determining the intensity and nature of the changes, and also examining the two typical modalities of representing the trend of change: linear and periodic models. Rainfall records were analyzed of the Córdoba Observatorio and Pilar Observatorio weather stations, as from 1910 and 1925 respectively, which belong to the Servicio Meteorológico Nacional (SMN) official network, and from a rain gauge located in Colonia Caroya, with data available as from 1929, that were selected by extension criteria, temporal integrity and geographical proximity. The non-parametric Mann-Kendall test (M-K) was used to identify the nature of the change, and the Theil-Sen (T-S) to evaluate intensity. These determine a significant linear trend ($P < 0.05$) in the region for total amount (PP) of rainfall, number of events (DPP), proportion of warm semester rainfall with respect to annual value, intensity (INT and PPmax) and variability, both annually and for the warm semester, when most of the annual rainfall occurs. However, adjusting these rainfall series to a simple sine function reveals a periodic behavior that explains a greater proportion of the observed variability with respect to the linear model, showing a negative phase of PP, DPP and PPmax during the period 1930–1950, which subsequently becomes positive between 1970 and 2000. Rainfall variability presents great dispersion in the region so neither the sine function nor the third-degree polynomial were appropriate to represent its long-term behavior. The linear trend loses statistical significance when the periodic behavior is incorporated into the analysis, leaving open the question about the influence of global warming on changes in the hydrological cycle and particularly on the rainfall regime in the central territory of Argentina.

1. Introduction

While climate change during the twentieth century has shown a sustained increase of atmospheric temperature on a global scale, the variation of the hydrological cycle components and, in particular, of rain, is more ambiguous and inconsistent. A first approach associated the influence of atmospheric heating on the hydrological cycle with the increase of the moisture-holding capacity of air (Allen and Ingram, 2002), increasing the quantity of precipitable water in the atmosphere. However, rainfall records do not always support this hypothesis (Huntington, 2011). Instead of producing an increase in mean rainfall values, global warming could be linked more to an increase in the frequency and intensity of rain events, as well as to their greater variability, both in time and space (Trenberth et al., 2003; Allan and Soden, 2008).

A variability analysis of the pluvial regime in a territory is necessary to project its potential impact, both on hydrological conditions in general, related to the excess and deficiency of water (Aragón et al., 2010; de la Casa and Nasello, 2015; Zhao et al., 2015), as well as on agricultural production, related to specific water use and the vulnerability of each farming activity (Todisco and Vergni, 2008; Viglizzo, 2010).

Rain is a meteorological phenomenon that is discontinuous in time and space, and therefore, to facilitate temporal analysis, variability is usually split into short-, medium- and long-term scales (Greene et al., 2011). Short-term variability depends on meteorological dynamics, modulated by the interaction of the atmosphere and the ocean, as in the El Niño Southern Oscillation (ENSO) among other processes (Chowdhury and Beecham, 2010; Rashid et al., 2014), and is expressed in periods ranging from hourly and daily to yearly fluctuations. Medium-term variability describes oscillations with cycles of between 10 and 20 years, associated with the dynamics of cosmic rays (de la Casa and Nasello, 2012), or the influence of climate controllers such as the Pacific Decadal Oscillation (PDO) (Mantua and Hare, 2002). Long-

* Corresponding author.
E-mail address: delacasa@agro.unc.edu.ar (A.C. de la Casa).

https://doi.org/10.1016/j.atmosres.2018.06.009
Received 10 April 2017; Received in revised form 7 June 2018; Accepted 8 June 2018
Available online 15 June 2018
0169-8095/ © 2018 Elsevier B.V. All rights reserved.

term variations, on the other hand, are those strictly related to climate change and, because they refer to a relatively permanent alteration of atmosphere in a region, their analysis requires not only prolonged and uninterrupted, but also reliable and consistent, time series data, to avoid misinterpretation (Dai et al., 1997; Costa and Soares, 2009).

In Argentina, de la Casa and Nasello (2010, 2012) reported a periodic behavior of the annual rainfall series in Córdoba province, using the non-linear method of Tomé and Miranda (2004). This cyclic scheme was also proposed for the southeast of La Pampa and the west of Buenos Aires provinces by different authors (Roberto et al., 1994; Pérez et al., 2003; Viglizzo, 2010).

A classical analysis procedure used to assess long-term climate change and variability is the Mann-Kendall (M-K) non-parametric method (Sneyers, 1990, 1997). Numerous studies worldwide have applied this methodology to establish the existence of change, its intensity, statistical significance and the nature of the variation. With the incorporation of a sequential or progressive variant, the M-K method has been extended to establish abrupt changes in series and the moment from which a possible modification occurs (Lázaro et al., 2001; Cislaghi et al., 2005; Liang et al., 2011; Soltani et al., 2013; Jones et al., 2015; Zhao et al., 2015). Rashid et al. (2015a, 2015b) identified trends in annual, seasonal and monthly rainfall in South Australia by using an approach combining a Continuous Wavelet Transform with the Mann Kendall test.

To assess the intensity of change in a time series, it is usual to employ the least squares (LS) technique, with the angular slope of the straight line expressing the sign and magnitude of change (Ravelo et al., 2003; Irmak et al., 2012). The Theil and Sen (T-S) method is a non-parametric procedure that also explains the linear evolution of a time series, with the advantage that its estimates are less affected by outlier data (Ohlson and Seil, 2014). Although the existence of a linear trend of a meteorological or hydrological variable can be recognized in the long term, a time series may show fluctuations during its evolution, so that the current condition differs markedly from what the linear model estimates. Thus, another way of expressing the temporal dynamics of a time series is to assume the periodic nature of the phenomenon, as suggested by Roberto et al. (1994), Pérez et al. (2003) and reaffirmed by Viglizzo (2010) for the west of Buenos Aires and La Pampa provinces in Argentina.

Given the secular scale of this analysis, rainfall variability must necessarily be evaluated in a long-term context, with the intrinsic difficulty of the existence and availability of time series over several years (Irmak et al., 2012). A long time series not only reveals the particular evolution of the climate system during that period, but is also necessary to assess the behavior of shorter data series (Villafuerte et al., 2014). The scarcity of rainfall data for central Argentina ostensibly reduces the number of stations that can provide useful records to evaluate the changes in rainfall during the last century. On the other hand, one way to sustain and verify the scope and certainty of changes detected in a pluvial regime is to examine the spatial coherence of the phenomenon: relatively close stations in a flat region should present similar behavior (Camargo and Hubbard, 1999).

Rainfall variations in a region can be manifested by changes in quantity, as well as by alterations in the frequency, intensity, seasonality or variability of these attributes (Rashid et al., 2015a, 2015b). Increases in the intensity of rainfall are potentially more dangerous because, with more abundant surface runoff and greater erosion capacity, they endanger not only productive but also environmental aspects (Kenyon and Hegerl, 2010; Willems et al., 2012; Porto De Carvalho et al., 2014; Villafuerte et al., 2014). An analysis of changes in rainfall intensity would be virtually impossible to perform from direct measurements because of the lack of long-term pluviographic records. This restriction is usually solved by using extreme value indicators constructed from more available daily rainfall data, such as maximum daily rainfall over a given period, the ratio of rainfall on wet days and the number of wet days, the highest rainfall value in 5 consecutive days, etc. (Alexander et al., 2006; Costa and Soares, 2009; Villafuerte et al., 2014; Limsakul and Singhruck, 2016; Rashid et al., 2016).

In view of the extension criteria, a potentially more rigorous and reliable analytical framework for long-term analysis that is compatible with a scale of climate change, even when the rain database is considerably reduced, includes temporal integrity, in relation to the continuity of the series over time, and geographic proximity, so that there is an instance of control or verification between registries. Also, although the concurrent requirement of these criteria reduces the number of viable cases for analysis, comparison between different sources of information provides valid support to sustain the long-term changes and to clarify the dynamics of rainfall fluctuations in a region.

The objective of this work was to evaluate in a secular context the variation of different attributes of the rainfall regime (quantity, frequency, seasonality, intensity and variability) in the central region of Argentina. More specifically, this involves determining the intensity and nature of the changes, using indicators to represent different characteristics of the pluvial phenomenon, to establish the evolution of the time series, and to analyze the local or regional character of these changes. Under current global warming conditions, this evaluation will ultimately provide evidence on the patterns of representation of rainfall variability in a long-scale framework, confronting the two main modes used to represent the temporal trend: linear and periodic models.

2. Materials and methods

2.1. Region of study and rainfall records used

The need to have long-term rainfall records in a reduced territory of the central region of Argentina significantly limited the availability of valid information for this study. The Servicio Meteorológico Nacional (SMN) of Argentina has two meteorological stations in this region that meet this requirement: Córdoba Observatorio (CO), located in Córdoba city and operated in the same place since its foundation in 1872; and Pilar Observatorio (PO), founded in the city of Pilar in 1904, with a precipitation series that extends from January 1, 1925 to the present day. As these weather stations are part of the World Meteorological Organization, they comply fully with international protocols of observation, recording and control, for which reason their rainfall data are considered as reference.

Additionally, daily data from a rain gauge in the town of Colonia Caroya (CC), 45 km north of Córdoba city, contain records uninterrupted from1 January 1929 until March 31, 2013. Fig. 1 shows the geographical location of these weather stations, which are in a flat territory with the mountain range of the Sierras Chicas of Córdoba to the west. The geographical location of the stations is completed with the detail of Table 1.

The series of rainfall records for CO was provided by the SMN and is from January 1, 1960 to December 31, 2012. In addition, to extend the database backwards, the number of rainy days per month was extracted from a publication with data ranging from January 1910 to December 1954 (Machado and Marchetti, 1955). Total monthly rainfall data were also obtained from the FAOCLIM 2 database records (FAOCLIM 2, 2001), which include complete monthly data for CO from January 1873 to December 1980. These records, duly updated, were previously used in a study about the recurrence of breakpoints in rainfall series in the province of Córdoba (de la Casa and Nasello, 2010).

2.2. Data processing and interpolation

Data from both PO and CC correspond to uninterrupted series of daily rainfall data. The information was added on annual (from January to December) and semi-annual time scales, establishing the warm semester (WS) between October of one year and March of the next, and the cold semester (CS) from April to September. The CC information exists in daily records only until March 2013, so the analysis of annual

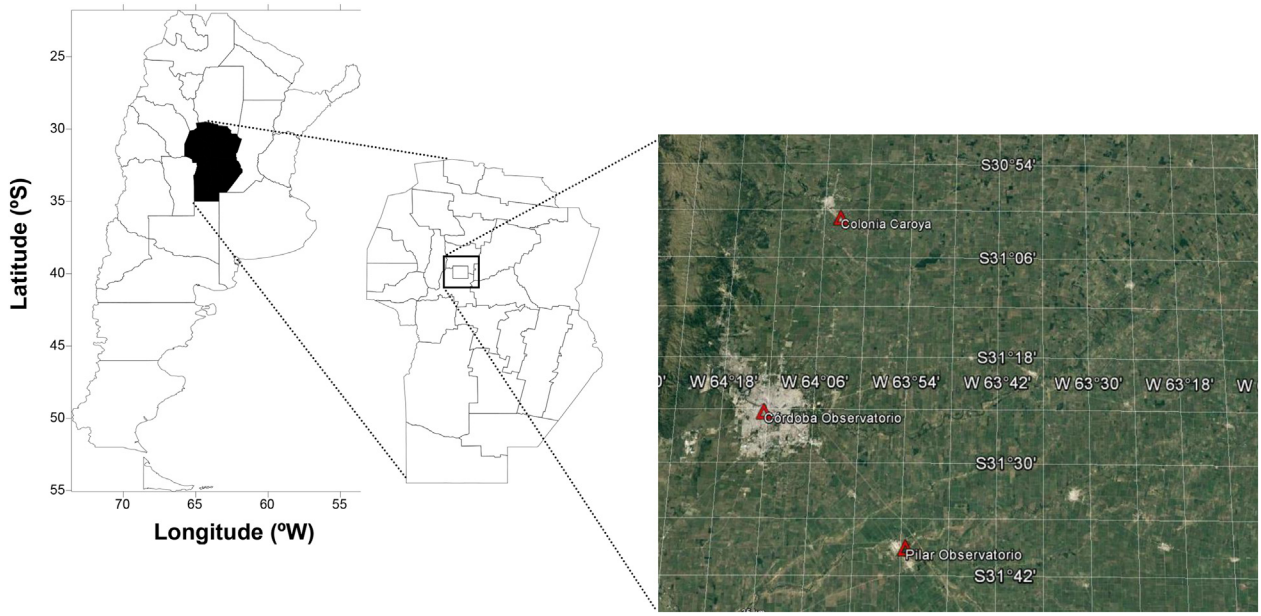

Fig. 1. Geographic location of Córdoba province in Argentina, with the meteorological stations used in this study on an image extracted from Google Earth.

Table 1
Detail of the geographical location, height and distance between weather stations.

Weather station	South latitude	West longitude	Height	Distance (km)		
			(m asl)	CO	PO	CC
Córdoba Observatorio (CO)	31° 24′	64° 11′	425		41	45
Pilar Observatorio (PO)	31° 40′	63° 53′	338	41		73
Colonia Caroya (CC)	31° 03′	64° 04′	477	45	73	

series was interrupted in 2012, while for WS the series was integrated with the data until 2013.

For CO, the total rainfall (PP) series of monthly values was integrated with the records of the FAOCLIM 2 (2001) database from 1910 to 1960 and, thereafter, with the SMN records. Since these were monthly values, it was not possible to evaluate intensity in terms of maximum daily value (PPmax).The series of rainy days per month (DPP) or monthly rainfall frequency used the records of Machado and Marchetti (1955) from 1910 to 1954, and information from the SMN since 1960. The lack of data between 1955 and 1960 was completed by an interpolation procedure which, for each month, estimated the rainy day frequency by a linear correlation and regression analysis between monthly rainfall data as an independent variable and rainy days for the period with previous data. The coefficients of the correlation and regression analysis are presented in Table 2.

2.3. Rainfall indices

The indicators used in the study to represent the rainfall regime were: total amount (PP), number of rainy days or frequency of events (DPP), mean intensity (PP/DPP), maximum daily value (PPmax), the variability of PP (PPCV) and DPP (DPPCV), which, for each period, was calculated as the quotient between the standard deviation and the mean value. In all cases, both the annual and semi-annual periods (WS and CS) were considered.

2.4. Homogeneity test

All time series were analyzed for homogeneity using the classical non-parametric Thom test, as Lázaro et al. (2001) did for rainfall records in Spain, and Nasri and Modarres (2009) for dry spells in Iran. For significance levels of $\alpha = 0.01$ and $\alpha = 0.05$, the null hypothesis of homogeneity is verified if $|Z| \leq 2.58$ and $|Z| \leq 1.96$, respectively. These results are given in Table 3.

2.5. Trend analysis

2.5.1. Methods for estimating linear trend

To evaluate trend behavior, in addition to the traditional least squares (LS) method, the non-parametric Mann-Kendall (M-K) and Theil-Sen (T-S) tests were also applied. While M-K analyzes only the existence of a trend, T-S explores its linear behavior. Calculations for statistical trend assessment were performed using the ProUCL 5.1 Software program (U.S. Environmental Protection Agency (EPA), 2016).

2.5.1.1. Mann-Kendall (M-K) test. This procedure has been used in

Table 2
Regression (a: Interception; b: Slope) and determination (R^2) coefficients of linear relationships to obtain the rainy days (DPP) from rainfall amount (PP) in each period for Córdoba Observatorio.

Coefficients	Jan	Feb	Mar	Apr	May	Jun	Jul	Aug	Set	Oct	Nov	Dec	Annual	WS	CS
a (day)	6.33	4.70	5.69	3.06	3.20	1.43	1.30	1.70	2.11	5.19	5.88	6.14	31.38	36.01	8.05
b (day mm^{-1})	0.03	0.03	0.03	0.05	0.03	0.15	0.07	0.07	0.07	0.03	0.03	0.03	0.06	0.03	0.09
R^2	0.33	0.32	0.17	0.39	0.20	0.51	0.33	0.36	0.47	0.29	0.17	0.44	0.56	0.24	0.59

References: WS and CS are the warm and cold semester, respectively

Table 3
Homogeneity test results of rainfall time series forweather stations used in this study.

Variable	Córdoba Observatorio					Pilar Observatorio					Colonia Caroya				
	R	E(R)	DE(R)	Z	p	R	E(R)	DE(R)	Z	p	R	E(R)	DE(R)	Z	p
PP Annual	48	51.91	4.99	0.78	0.433	43	44.43	4.60	0.31	0.756	40	42.90	4.54	0.64	0.523
PP WS	45	52.38	5.04	1.46	0.143	37	42.73	4.42	1.30	0.195	36	42.14	4.46	1.38	0.168
PP CS	49	51.91	4.99	0.58	0.560	41	44.18	4.58	0.70	0.487	43	42.90	4.54	0.02	0.983
DPP Annual	31	52.38	5.04	4.24	***0.000***	43	44.80	4.64	0.39	0.699	27	43.00	4.55	3.51	***0.000***
DPP WS	31	51.10	4.91	4.09	***0.000***	34	44.91	4.65	2.34	***0.019***	31	42.90	4.54	2.62	***0.009***
DPP CS	35	52.50	5.05	3.47	***0.001***	46	44.98	4.66	0.22	0.826	41	41.07	4.34	0.02	0.987
INT Annual	52	52.50	5.05	0.10	0.922	38	44.91	4.65	1.48	0.138	30	42.90	4.54	2.84	***0.005***
INT WS	48	52.38	5.04	0.87	0.385	42	44.98	4.66	0.64	0.523	46	42.79	4.53	0.71	0.478
INT CS	43	52.26	5.03	1.84	0.065	47	44.64	4.62	0.51	0.609	46	42.98	4.55	0.66	0.507
PPmax Annual						38	43.89	4.54	1.30	0.195	42	42.90	4.54	0.20	0.842
PPmax WS						38	43.89	4.54	1.30	0.195	38	42.79	4.53	1.06	0.291
PPmax CS						39	43.89	4.54	1.08	0.282	39	42.79	4.53	0.84	0.403
CV PP Annual	55	51.91	4.99	0.62	0.536	44	44.80	4.64	0.17	0.864	38	41.07	4.34	0.71	0.479
CV PP WS	51	52.46	5.05	0.29	0.773	46	44.64	4.62	0.29	0.768	45	41.83	4.43	0.72	0.474
CV PP CS	50	51.91	4.99	0.38	0.702	40	45.00	4.66	1.07	0.284	43	42.98	4.55	0.01	0.996
CV DPP Annual	49	52.11	5.01	0.62	0.535	45	44.98	4.66	0.00	0.996	44	41.83	4.43	0.49	0.625
CV DPP WS	57	51.91	4.99	1.02	0.308	47	44.98	4.66	0.43	0.664	43	41.83	4.43	0.26	0.792
CV DPP CS	49	51.68	4.97	0.54	0.590	54	44.98	4.66	1.94	0.053	37	40.62	4.29	0.84	0.399

References: R: number of runs; E(R): average; DE(R): Standard Deviation; Z: statistic; p: probability ($p < 0.01$ in bold and cursive)

hydrology and climatology to analyze randomness against trend of time series. As it is a rank-based procedure, it is robust to the influence of extremes and a good test for skewed data. For any sample of n variables, $x_1, \ldots, x_n$, the null hypothesis states that the samples are independent and identically distributed. The alternative hypothesis of a two-sided test is that the distributions of x_i and x_j are not identical for all $i, j \leq n$ with $i \neq j$.

The M-K test is based on the statistic S, which is calculated as follows:

$$S = \sum_{i=2}^{n} \sum_{j=1}^{i-1} sign(x_i - x_j)$$

where x_i and x_j are the annual values of rainfall index in years i and j, $j > i$, respectively, and sign $(x_i - x_j)$ is -1 for $(x_i - x_j) < 0$; 0 for $(x_i - x_j) = 0$, and 1 for $(x_i - x_j) > 0$.The mean $E[S]$ and variance $V[S]$ of the statistic S may be given as:

$$E[S] = 0$$

$$V[S] = \frac{n(n-1)(2n+5) - \sum_{p=1}^{q} t_p(t_p-1)(2t_p+5)}{18}$$

where t_p is the number of ties for the p_{th} value and q is the number of tied values. The second term represents an adjustment for tied or censored data. The standardized test statistic ($Z_{M\text{-}K}$) is computed by:

$$Z_{M-K} = \begin{cases} \frac{S-1}{\sqrt{V(S)}} & \text{if } S > 0 \\ 0 & \text{if } S = 0 \\ \frac{S+1}{\sqrt{V(S)}} & \text{if } S < 0 \end{cases}$$

While a positive $Z_{M\text{-}K}$ indicates an increasing trend, a negative $Z_{M\text{-}K}$ indicates a decreasing trend. To test for either an increasing or a decreasing monotonic trend at p significance level, the null hypothesis is rejected if the absolute value of Z is greater than $Z_{1-p/2}$, where $Z_{1-p/2}$ is obtained from the standard normal cumulative distribution tables. In this work, different significance levels of p (0.1; 0.05 and 0.01) were applied.

2.5.1.2. Theil-Sen (T-S) test. Two methods were applied for estimating the linear trend of the time series: the least squares (LS) classic method and the non-parametric Theil-Sen technique (T-S), which is assigned more robust behavior as this is less affected by the occurrence of outliers. As defined by Theil (1950), the Theil-Sen estimator of a set of two-dimensional points (x_i,y_i) is the median m of the slopes $(y_j - y_i)/(x_j - x_i)$ determined by all pairs of sample points. Sen (1968) extended this definition to handle the case in which two data points have the same x-coordinate. Sen's definition takes the median of the slopes defined only from pairs of points having distinct$x$-coordinates. Once the slope m has been determined, a line is determined from the sample points by setting the y-intercept b to be the median of the values $y_i - mx_i$.

To analyze temporal trends, the hypotheses tested were:

I. Null hypothesis (H0): Data set does not exhibit sufficient evidence of any trends (stationary measurements) vs.:
II. Alternative hypothesis (HA): Data set exhibits a trend (two-sided alternative):
   i. Data set exhibits an upward trend; or
   ii. Data set exhibits a downward trend.

Case 1. Testing H0: Time series data set does not exhibit any trend, vs. the two-sided alternative hypothesis, HA: Data set exhibits a trend. First, a critical value Cα is calculated using the following equation:

$$C\alpha = Z_{\alpha/2} sd(S)$$

and then M_1 and M_2 are computed as:

$$M_1 = \frac{N - C_\alpha}{2}; \qquad and\ M_2 = \frac{N + C_\alpha}{2}$$

The 1st largest M and 2nd largest M slopes, $m_{(M1)}$ or LCL, and $m_{(M2)}$ or UCL, are obtained from the set consisting of all $n(n-1)/2$ slopes. Then the probability of the T-S slope, Q, lying between these two slopes is given by:

$$P(m_{(M1)} < Q < m_{(M2)}) = 1 - \alpha$$

If 0 belongs to the interval, $(m_{(M1)}, m_{(M2)})$, then the T-S test slope is insignificant; that is, there is no significant trend present in the time series data set.

Case 2. Test for an upward (downward) trend with H0: Time series data set does not exhibit any trend, vs. HA: data set exhibits an upward (downward) trend.

Once the 1st largest M and 2nd largest M slopes, $(m_{(M1)})$ and $(m_{(M2)})$, from all $n(n-1)/2$ slopes are obtained: If $(m_{(M1)}) > 0$, then the data set exhibits a significant upward trend, and if $(m_{(M2)}) < 0$, then the data

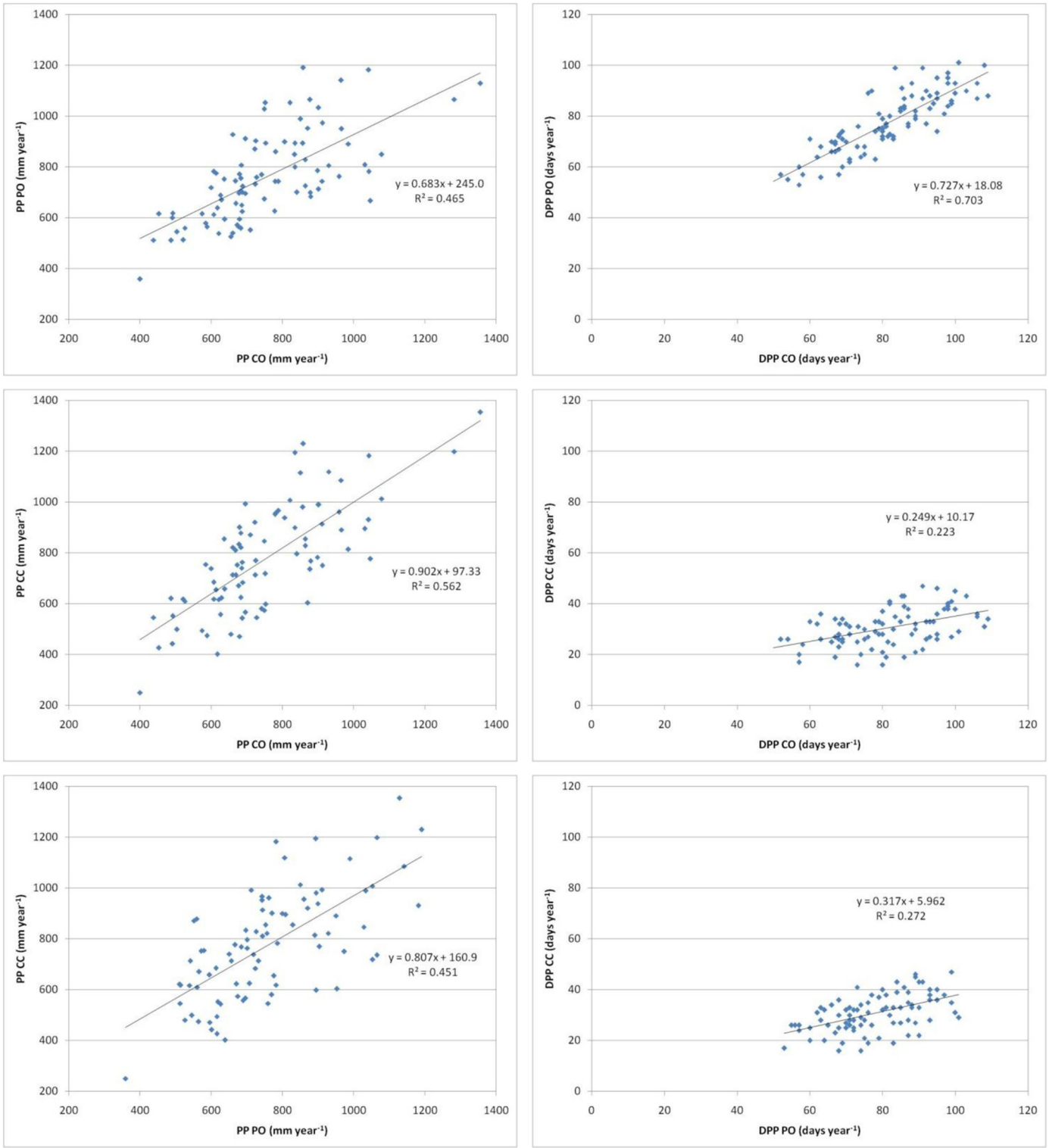
PP PO (mm year⁻¹)
PP CO (mm year⁻¹)
y = 0.683x + 245.0
R² = 0.465
DPP PO (days year⁻¹)
DPP CO (days year⁻¹)
y = 0.727x + 18.08
R² = 0.703
PP CC (mm year⁻¹)
PP CO (mm year⁻¹)
y = 0.902x + 97.33
R² = 0.562
DPP CC (days year⁻¹)
DPP CO (days year⁻¹)
y = 0.249x + 10.17
R² = 0.223
PP CC (mm year⁻¹)
PP PO (mm year⁻¹)
y = 0.807x + 160.9
R² = 0.451
DPP CC (days year⁻¹)
DPP PO (days year⁻¹)
y = 0.317x + 5.962
R² = 0.272

Fig. 2. Relationships for annual values of total rainfall (PP) and rainy days (DPP) between Córdoba Observatorio (CO), Pilar Observatorio (PO) and Colonia Caroya (CC) weather stations.

set exhibits a significant downward trend.

2.5.2. Evaluation of the periodic behavior

To represent the periodic behavior of precipitation, a sine function was used, which is a formally simple model and requires few adjustment coefficients. The generic expression of the function used is:

$$Y_{year} = \overline{Y} + A \times \sin(P \times t)$$

where Y_{year} is the rainfall index (PP, DPP, PPmax, etc.) estimated each year; $\bar{Y}$ is the mean value for the series; A is the amplitude; P is the period ($2\pi/B$); t is the time dimension, with values between 0 and 1, that was calculated as $t = (year\text{-}year_{initial}) / (year_{final} - year_{initial})$. Parameters A and B are the coefficients of the model that were determined by means of non-linear adjustment.

3. Results and discussion

3.1. Relationship between rainfall records in the central region of Argentina

The results of Fig. 2 show the close relationship between the rainfall data recorded in the stations of central Argentina during the long period analyzed, both when considering the annual total amount (PP) and the number of rainy days (DPP) per year. This uniform behavior of rainfall is justified because these are relatively close stations in flat territory. Although the correlation between meteorological variables tends to decrease sharply with distance, and particularly in the case of daily rainfall (Camargo and Hubbard, 1999), the annual step of rainfall series in this case maintains a high level of correlation ($r = 0.67$) up to 73 km, the distance separating PO from CC. This correlation is slightly lower than the value observed for the smaller distances between CO and CC ($r = 0.75$), or between CO and PO ($r = 0.68$). The same study of the annual frequency of events, however, indicates that recording of rainy days in CC is significantly lower than in both stations of the SMN used in this study.

Although with some noticeable differences between records, the annual rainfall frequency recorded in the SMN stations, CO and PO, tends to be similar, with a correlation (r) of 0.84 and a slope of 0.73, a value approaching 1. The annual frequency of rainfall in CC not only produces lower correlations with respect to the SMN weather stations ($r = 0.47$ with CO and $r = 0.52$ with PO), but its number of rainy days per year is also notably lower. This discrepancy indicates that the observation regime of the CC rain gauge does not strictly comply with the norms established by the official registration system to identify a rainy day, as evidenced by not finding values below 1 mm in its database. However, since the annual amount of rainfall at the stations is similar (the mean values of CO and PO are not statistically different from those of CC ($P > 0.05$) in the period 1929–2012), it is likely that the criteria of measurement and recording in CC is more per event (on consecutive days) than per day of rain. As Table 3 shows, homogeneity is verified for almost all the rainfall records analyzed, except for the rainy days. While the interpolation procedure in CO could explain this lack of homogeneity, in CC it is very likely due to this observational problem.

3.2. Changes in total amount of rainfall

Fig. 3 presents the variation of the total amount of rain in the warm and cold semesters in CO, PO and CC throughout the study period. The graphs show that rainfall is seasonally very homogeneous in the region, with a greater supply during the warm semester (WS). While each day of rain in CO during the WS contributes 9.4 mm, this is reduced by half during the CS. Thus, the amount of rain accumulated from October to March is well above the total of the cold semester in all 3 stations, with a range of between approximately 400 and 800 mm. A systematic long-term increase over time is observed for the WS, as the linear functions show using both LS and T-S methods.

As indicated in Table 4, this increasing trend of yearly values reaches statistical significance ($P < 0.05$) at the 3 sites when it is evaluated by M-K, and also in the warm semester (WS). T-S, on the other hand, does not validate the significance of the trend at PO either annually or semi-annually. Otherwise, during the period, precipitation in CS is stable for all three sites, with values that generally do not exceed 200 mm and that show no evidence of having changed during the century. This seasonal lack of rainfall between April and September and its greater interannual variability, with coefficients of variation that double the annual and WS values (Table 4), is a very representative climatic feature of the region, and is a major limiting factor for rainfed crop production, like wheat (de la Casa et al., 2004).

The linear functions that are determined from both LS and T-S are also very similar in both semesters, as shown in Fig. 3, with respective slopes expressing the character and intensity of the change. Due to its more robust behavior when outlier data are presented, such as cases above 1200 mm recorded during 1977 in both PO and CC, it seems appropriate at both sites to consider the slightly lower slope estimated by the T-S method.

3.3. Changes in rainfall frequency

Rain processes in the region increase during the warm season of the year. Analyzing the interannual variation in the number of rainy days on a semiannual scale, Fig. 4 represents the rainfall behavior, restricted only to stations in the official network (CO and PO) to avoid considering the abnormality of the CC measurements (Fig. 2). Both stations show a frequency in the WS that doubles CS values and, in addition, an increasing long-term trend. The linear functions obtained with LS and T-S procedures describe the long-term increase in a very similar way, and this is significant ($P < 0.05$), both in the WS and in the annual series, according to the results of the M-K and T-S tests (Table 5).

Only at CO is there a significant increase in the number of rainy days during the CS. In this case, the increase in the total amount of rain accompanied by a greater number of events shows, in the first instance, a similar average intensity of rain over time. On the other hand, at PO, rain during the CS shows, apart from the great interannual variability that is common in the region, consistent behavior over time, both in quantity and in its frequency.

3.4. Changes in the seasonal regime of rainfall

As in most of northwest Argentina, precipitation in the region under study has a typical monsoon behavior, with more intense and more frequent events during the WS, when tropical convection conditions settle over South America (González and Barros, 1998). The classical taxonomic system of Köppen-Geiger qualifies the climate as dry in winter in this region (Peel et al., 2007). Assessing rainfall in the warm and cold semesters in relation to the total amount is a way to determine the seasonal behavior of the rainfall, projecting this water contribution for the summer and winter crops in the region. In this way, the seasonal variation over time would express a modification of rainfall that would potentially have a direct impact on rainfed agriculture in the territory. The analysis of seasonal rainfall variability is presented graphically in Fig. 5, considering the total amounts and the frequency of events separately.

Fig. 5 shows seasonal rainfall to be homogeneous in the region, both in the amount of accumulated water and in the number of rainy days. Considering total rainfall, the three sites show very consistently that the WS contributes approximately 80% of the annual total, with a slight increasing trend, although it reaches statistical significance ($P < 0.05$) only at CO. On the other hand, rainfall in CS tends to systematically, but not significantly, decrease implying that winter periods would currently be slightly drier. Although the difference between the contribution of each semester tends to increase, the persistence of this feature of the rain during the long period analyzed is remarkable, which confers a structural climatic character and supports the taxonomic category of Köppen-Geiger as dry in winter for this region.

This same seasonality is evidenced by the frequency of events but, in this case, with a clear difference between the official weather stations and CC. While the frequency of events in CS (WS) with respect to the annual total is slightly higher (lower) in both CO and PO, contributing about 30% (70%) of annual events, in CC the percentage is reduced (increased) to 20% (80%). This difference is explained, according to the information in Fig. 2, by the particular observational regime at CC in which fewer rainy days were systematically recorded. Comparing the methods used to depict the trend line and to have a measure of the intensity of the change over time, it is noticeable that the LS adjustment and the non-parametric T-S method both produce very similar results.

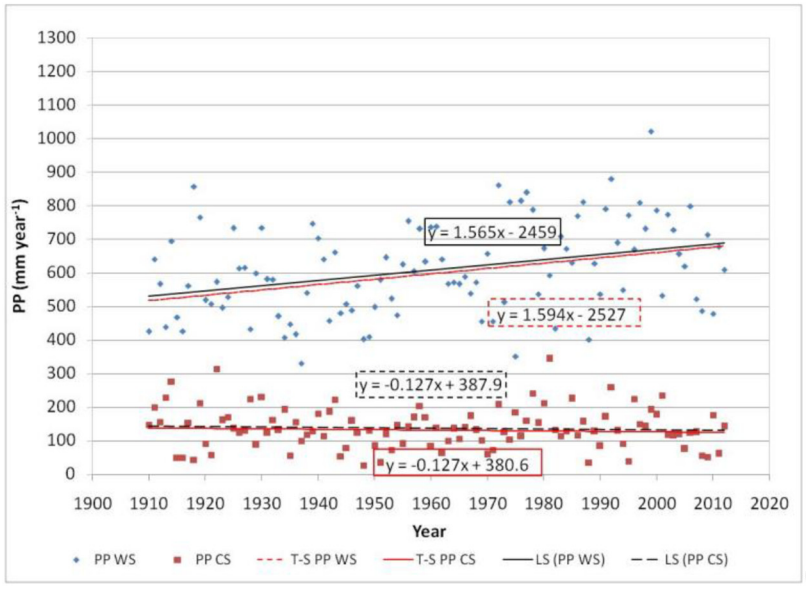

(a)

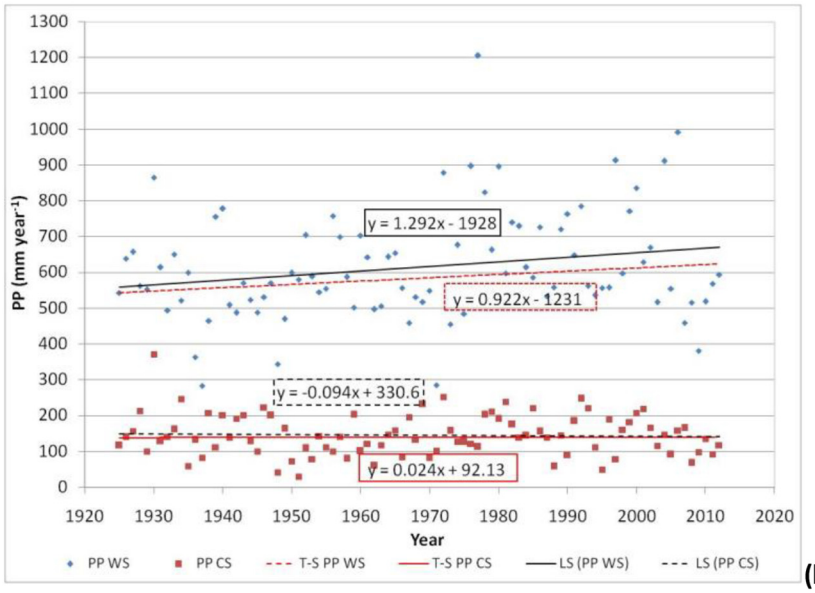

(b)

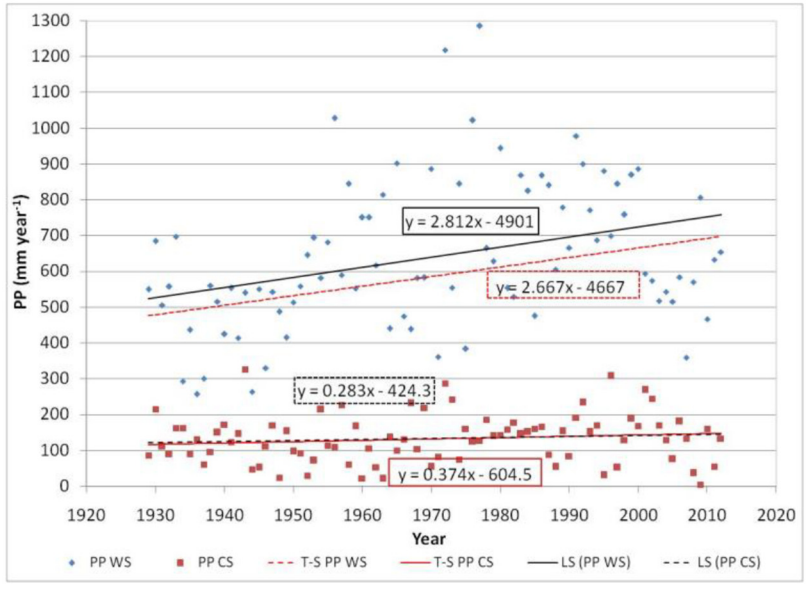

(c)

(caption on next page)

Fig. 3. Interannual variation of rainfall amount in the warm (PP WS) and cold (PP CS) semesters in Córdoba Observatorio (a), Pilar Observatorio (b) and Colonia Caroya (c) weather stations. Also, trend lines obtained by least squares (LS) (black) and the non-parametric method of Theil-Sen (T-S) (red) are presented, as well as the adjustment functions for the respective semesters. (For interpretation of the references to colour in this figure legend, the reader is referred to the web version of this article.)

3.5. Changes in intensity of rainfall

The long-term variation of rainfall intensity is analyzed, firstly, considering the quotient between the amount of rainfall and the number of events. The mean intensity (INT) at annual and semi-annual levels is presented in Table 6.

As indicated in Table 6, statistical tests at CC show a growing and significant trend of INT in both the annual and semi-annual periods, which, as mentioned, can be explained by the significant PP increase in the absence of a DPP change. The significant difference in rainy days between CC and the official meteorological stations greatly limits the scope of this information and puts in doubt that it corresponds to a real modification. INT at CC presents average annual and semi-annual values that duplicate those of CO and PO. In contrast, the general tendency of INT at CO and PO is to decrease but, while the trend is not significant at PO, at CO the decrease is significant during the cold semester, as a consequence of the increase of DPP.

Another more direct way of evaluating long-term changes in rainfall intensity is to use an indicator such as the maximum daily value over a given period. This analysis, as shown in Table 7, was restricted to PO and CC as only these stations have daily rainfall records for all the period.

The trend evaluation of PPmax shows some differences between the weather stations according to the analytical method used. At PO, only the M-K test shows significance for the increasing trend of annual and WS rain intensity, but at a slightly lower level of confidence ($P < 0.10$). Instead, at CC both methods used support an increase of rain intensity, for both annual and semiannual values. This is important as it indicates a growing environmental and productive risk today as a result of more intense rains (Porto De Carvalho et al., 2014; Villafuerte et al., 2014). However, this analysis would be incomplete if the evolution of the trend over time is not considered.

3.6. Changes in rainfall variability

A less explored aspect of changes in rainfall is the modification of variability over time. A classic indicator of variability is the coefficient of variation determined for each year or semester from monthly values of the amount of rainfall and the number of events. Tables 8 and 9 present a synthesis of the trends of variability of total rainfall and of rainy days, respectively.

With respect to the change in variability of total rainfall over time, the annual series of the official network shows a significant increasing trend, evident in both M-K and T-S. On the other hand, the trend analysis of variability of the annual frequency of events shows only a significant decrease at CC when using the M-K method for the WS series and, with less confidence, for the annual series. Anyway, by the previous analysis, this would not be totally reliable.

3.7. Trend of the rainfall regime: linear increase or periodic variation

The information in Tables 4 and 5 supports the existence of a growing linear trend in rainfall series for both total amount (PP) and number of rainy days (DPP). These changes can be considered general in the region since, with the limitations of the case due to the lower number of rainy days recorded in CC (Fig. 2 and Fig. 6), the time series of these attributes show a very similar behavior at the three sites. Not only does the classical M-K method support the existence of a trend in the region, but the T-S procedure also validates a progressive increase in the amount and frequency of rainfall in a secular scale, so the evidence of this linear increase is statistically significant (Dai et al., 1997; Trenberth et al., 2007; Courtillot et al., 2013).

Fig. 6, however, presents the variation overtime of PP and DPP for stations in the central region, and incorporates the sine functions obtained by empirical adjustment to the respective annual rainfall series from the coefficients in Table 10. A simple sine function was used by Roberto et al. (1994) and Pérez et al. (2003) to represent the periodic variation of rain in the La Pampa and Buenos Aires provinces of Argentina, and is very similar to 3rd degree polynomial functions. Table 10 presents the regression and correlation coefficients (R^2) of the sinusoidal and polynomial models, to compare them with the respective coefficients of the linear model.

At all three sites, the sine functions accurately describe the periodic rainfall behavior for both PP and DPP, with waves that show contemporaneously a negative rainfall anomaly during the first period of the analysis, which changes to positive afterward between the 1960s and 1990s, and again to a negative anomaly lately (Glave, 2006; Carreño and Viglizzo, 2011; de la Casa and Ovando, 2014). The greater adjustment of the periodic function with respect to the linear model, which approximately doubles the proportion of explained variance of rainfall time series, as shown in Table 10, constitutes a serious objection to the relevance of the linear representation for indicating future rainfall change.

Moreover, this evidence rejects the hypothesis of a modification of the hydrological cycle for central Argentina and, in particular, that the rainfall regime is influenced by atmospheric warming resulting from

Table 4
Trend analysis of the Mann-Kendall (M-K) and Theil-Sen (T-S) tests for the annual and seasonal values (warm (WS) and cold semester (CS)) of total rain amount (PP) of weather stations used in this study.

	Córdoba Observatorio			Pilar Observatorio			Colonia Caroya		
	Annual	WS	CS	Annual	WS	CS	Annual	WS	CS
Number of events	103	103	103	88	88	88	84	84	84
Mean	747.2	610.2	137.5	759.7	615.3	145.2	775.2	641.1	133.2
Coefficient of variation	0.229	0.224	0.449	0.23	0.25	0.401	0.275	0.321	0.512
M-K test value (S)	876	1176	−203	491	481	28	903	838	330
Standardized value of S	2.493	3.348	−0.576	1.766	1.73	0.0973	3.485	3.234	1.271
Approximate *p*-value	0.00633	4.07E-04	0.282	0.0387	0.0418	0.461	2.46E-04	6.11E-04	0.102
Number of slopes	5253	5253	5253	3828	3828	3828	3486	3486	3486
M1′	2338	2338	2283	1642	1642	1642	1530	1530	1489
One-sided 95% lower limit of slope	0.414	0.878	2970	2186	2186	2186	1.87	1.227	1997
95% LCL of slope (0.025)	0.267	0.703	−0.535	−0.167	−0.098	−0.478	1.626	1.0	−0.232
95% UCL of slope (0.975)	2.228	2.5	0.292	2.737	2.037	0.463	5.32	4.382	1.0

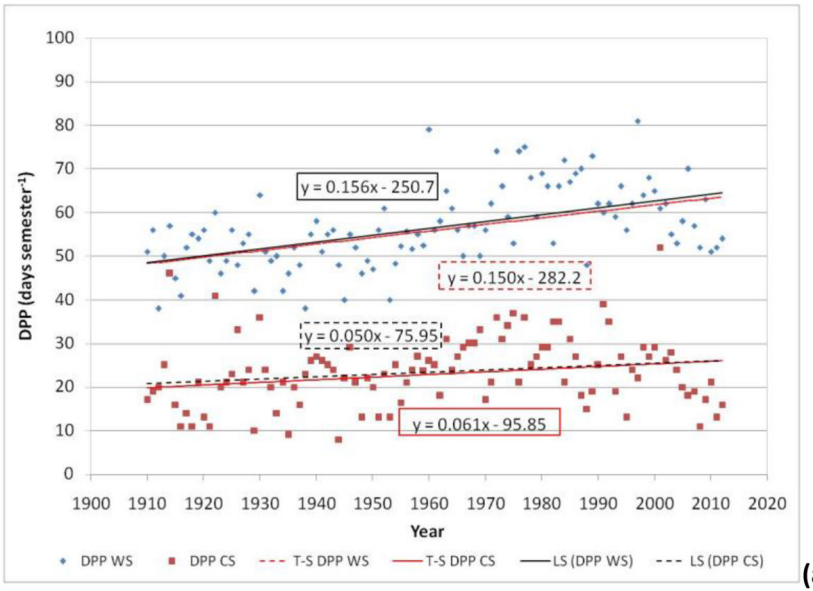

Fig. 4. Interannual variation of the number of rainy days (DPP) in the warm (WS) and cold (CS) semesters in Córdoba Observatorio (a) and Pilar Observatorio (b). The trend lines obtained by least squares (LS) (black) and the non-parametric method of Theil-Sen (T-S) (red) are presented, as well as the adjustment functions for the respective semesters. (For interpretation of the references to colour in this figure legend, the reader is referred to the web version of this article.)

Table 5
Trend analysis of the Mann-Kendall (M-K) and Theil-Sen (T-S) tests for the annual and seasonal values (warm (WS) and cold semester (CS)) of rainy days (DPP) for the weather stations used in this study.

	Córdoba Observatorio			Pilar Observatorio			Colonia Caroya		
	Annual	WS	CS	Annual	WS	CS	Annual	WS	CS
Number of events	103	103	103	88	88	88	84	84	84
Mean	80.14	56.49	23.5	77.55	54.2	23.43	30.6	24.38	6.167
Coefficient of variation	0.175	0.158	0.343	0.152	0.148	0.282	0.238	0.265	0.526
M-K test value (S)	1529	1925	810	854	951	89	224	253	−188
Standardized value of S	4.356	5.488	2.308	3.076	3.43	0.318	0.863	0.975	−0.729
Approximate p-value	6.62E-06	2.03E-08	0.0105	0.00105	3.02E-04	0.375	0.194	0.165	0.233
Number of slopes	5253	5253	5253	3828	3828	3828	3486	3486	3486
M1′	2338	2338	2338	1686	1686	1643	1490	1490	1492
One-sided 95% lower limit of slope	0.138	0.106	0.0139	0.0833	0.0642	2185	1996	1996	1994
95% LCL of slope (0.025)	0.126	0.0976	0	0.0606	0.0526	−0.043	−0.041	−0.029	−0.031
95% UCL of slope (0.975)	0.31	0.203	0.112	0.27	0.185	0.0625	0.1	0.0938	0

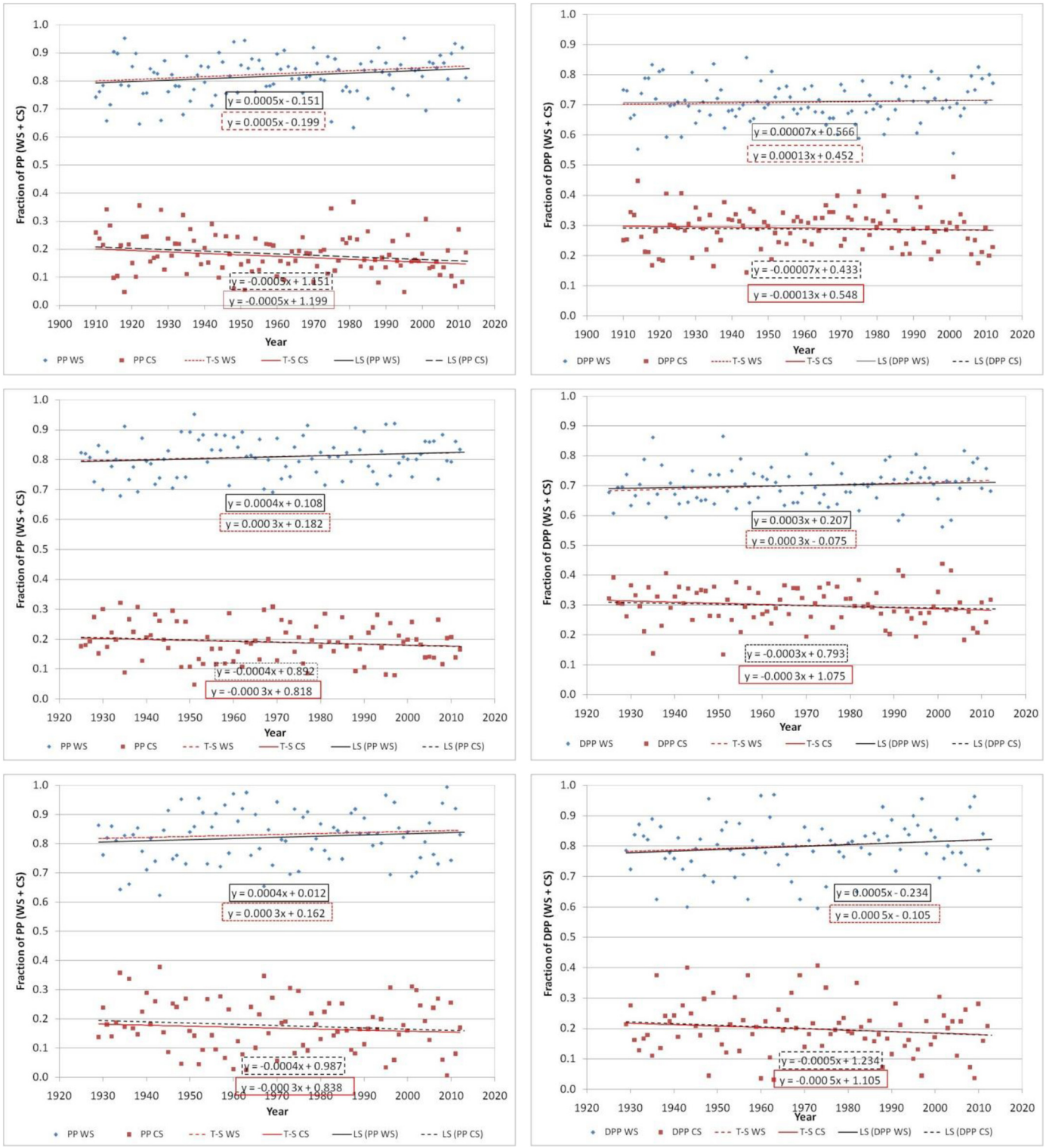

Fig. 5. Interannual variation of total rainfall (PP, left) and rainy days (DPP, right) in the warm (WS) and cold (CS) semesters relative to the total value (WS + CS) for Córdoba Observatorio (above), Pilar Observatorio (middle) and Colonia Caroya (below). The figures show the trend lines obtained by least squares (LS) (black) and by the non-parametric method of Theil-Sen (T-S) (red), as well as the respective adjustment functions. (For interpretation of the references to colour in this figure legend, the reader is referred to the web version of this article.)

the steady increase of CO_2 concentrations during the 20th and early 21st century (Trenberth et al., 2007; Huntington, 2011). Global warming's influence on rainfall does not yet have a convincing and much less a generalized explanation. While Killam et al. (2014) observe an increase of precipitation in California (USA), concentrated in the north of the state, the change in the south is insignificant, with even a decrease of rain verified since the 1970s. In addition, rainfall intensity has not changed significantly with global warming; in Sacramento (to the north), there is a greater amount and frequency of rain, but its intensity is lower. On the other hand, Los Angeles (to the south) shows greater intensity of rain, but decreasing rainy days and total amounts. Zhao et al. (2015), meanwhile, detected a decrease in rainfall and

Table 6
Trend analysis of Mann-Kendall (M-K) and Theil-Sen (T-S) tests for the annual and seasonal values (warm (WS) and cold semester (CS)) of mean rainfall intensity (INT) for the weather stations used in the study.

	Córdoba Observatorio			Pilar Observatorio			Colonia Caroya		
	Annual	WS	CS	Annual	WS	CS	Annual	WS	CS
Number of events	103	103	103	88	88	88	84	84	84
Mean	9.363	10.84	5.933	9.818	11.4	6.263	25.65	26.6	22.74
Coefficient of variation	0.172	0.18	0.359	0.185	0.215	0.337	0.214	0.237	0.399
M-K test value (S)	−477	−177	−970	−104	−152	−202	1132	840	539
Standardized value of S	−1.356	−0.502	−2.761	−0.371	−0.544	−0.724	4.369	3.241	2.079
Approximate p-value	0.0875	0.308	0.00288	0.355	0.293	0.234	6.24E-06	5.95E-04	0.0188
Number of slopes	5253	5253	5253	3828	3828	3828	3486	3486	3486
M1′	2283	2283	2915	1642	1642	1642	1530	1530	1530
One-sided 95% lower limit of slope	2970	2970	−0.0093	2186	2186	2186	0.0707	0.0461	0.0165
95% LCL of slope (0.025)	−0.0179	−0.0164	−0.0352	−0.0189	−0.0259	−0.0233	0.0626	0.0368	0.00374
95% UCL of slope (0.975)	0.00289	0.0109	−0.00697	0.012	0.0137	0.0119	0.156	0.145	0.157

Table 7
Trend analysis of Mann-Kendall (M-K) and Theil-Sen (T-S) tests for the annual and seasonal values (warm (WS) and cold semester (CS)) of maximum daily rainfall (PPmax) for Pilar Observatorio and Colonia Caroya weather stations.

	Pilar Observatorio			Colonia Caroya		
	Annual	WS	CS	Annual	WS	CS
Number of events	88	88	88	84	84	84
Mean	72.5	69.64	39.9	88.99	85.52	47.49
Coefficient of variation	0.31	0.347	0.467	0.306	0.339	0.446
M-K test value (S)	467	423	147	1066	920	556
Standardized value of S	1.68	1.521	0.526	4.116	3.551	2.145
Approximate p-value	0.0465	0.0641	0.299	1.93E-05	1.92E-04	0.016
Number of slopes	3828	3828	3828	3486	3486	3486
M1′	1642	1642	1642	1530	1530	1530
One-sided 95% lower limit of slope	2186	2186	2186	0.294	0.23	0.0431
95% LCL of slope (0.025)	−0.0277	−0.04	−0.0987	0.26	0.189	0.0132
95% UCL of slope (0.975)	0.344	0.347	0.178	0.667	0.667	0.393

runoff between 1960 and 2010 in the Wei River Basin, the main tributary of the Yellow River (Huang He) in China. Jones et al. (2015) found that, at 41 (37) of the 78 stations analyzed in the Upper Tennessee Valley (USA), annual precipitation increased (decreased) between 1950 and 2009, but only 7 negative and 2 positive rates were statistically significant.

To represent the long-term periodic behavior, despite comparing series of different lengths, the sine function is analytically effective visual expression to describe the wave dynamics of rainfall. From more specific analysis techniques, different authors have proposed this cyclical behavior to represent the variation of air surface temperature during the 20th century, with an oscillation of 60 years, very close to that shown by the rain series in this region (Klyashtorin et al., 2009; Scafetta, 2010; Lyubushin and Klyashtorin, 2012; Courtillot et al., 2013). The oscillation shown in Fig. 6, moreover, also explains the increasing linear trend of rain during the last 50–60 years of the 20th century, an increase that until then had validated the influence of global warming on rainfall in the central region of Argentina (Viglizzo et al., 1995; Lucero and Rozas, 2002; de la Casa and Nasello, 2010). When the time series extends over a (quasi) secular period, the transition from a relatively dry period during the 1930s, 1940s and 1950s, to a more humid stage between 1970 and 2000, accounts for the increase in the linear trend. However, it is likely that the greater extent of the wet phase justifies the results supporting the existence of an increasing linear trend for rainfall series throughout the entire period analyzed.

From the PPmax index, the previous analysis also showed a progressive increase in rainfall intensity that is particularly consistent at CC because it manifests equally during the warm and cold semesters, and according to both methods used to evaluate the trend, and is also insinuated at PO from the M-K method (Table 7). However, Fig. 7 presents the time series of annual values of PPmax for both stations and the respective sine functions that were obtained by fit. Again, in this case, although rainfall intensity shows a growing linear trend in the region that the analytical methods support statistically (Table 7), visual inspection of Fig. 7 shows the existence of a long-term fluctuation, in

Table 8
Trend analysis of Mann-Kendall (M-K) and Theil-Sen (T-S) tests for the annual and seasonal values (warm (WS) and cold semester (CS)) of total rain variability (PPCV) for the weather stations used in the study.

	Córdoba Observatorio			Pilar Observatorio			Colonia Caroya		
	Annual	WS	CS	Annual	WS	CS	Annual	WS	CS
Number of events	103	103	103	88	88	88	84	84	84
Mean	0.958	0.528	1.213	0.936	0.527	1.181	1.061	0.795	1.508
Coefficient of variation	0.162	0.303	0.287	0.163	0.318	0.297	0.173	0.186	0.315
M-K test value (S)	755	127	139	608	476	416	246	−12	−13
Standardized value of S	2.149	0.359	0.393	2.188	1.712	1.496	0.946	−0.0425	−0.0464
Approximate p-value	0.0158	0.36	0.347	0.0143	0.0435	0.0674	0.172	0.483	0.482
Number of slopes	5253	5253	5253	3828	3828	3828	3486	3486	3486
M1′	2338	2283	2283	1686	1642	1642	1489	1489	1489
One-sided 95% lower limit of slope	0.0003	2970	2970	0.0004	2186	2186	1997	1997	1997
95% LCL of Slope (0.025)	0.0001	−0.0010	−0.0019	0.0001	−0.0002	−0.0006	−0.0007	−0.0015	−0.0041
95% UCL of Slope (0.975)	0.0021	0.0013	0.0028	0.0025	0.0025	0.0054	0.0021	0.0013	0.0041

Table 9
Trend analysis of Mann-Kendall (M-K) and Theil-Sen (T-S) tests for the annual and seasonal values (warm (WS) and cold semester (CS)) of rainy day variability (DPPCV) for the weather stations used in the study.

	Córdoba Observatorio			Pilar Observatorio			Colonia Caroya		
	Anual	WS	CS	Anual	WS	CS	Anual	WS	CS
Number of events	103	103	103	88	88	88	84	84	84
Mean	0.622	0.315	0.749	0.606	0.326	0.709	0.939	0.697	1.361
Coefficient of variation	0.197	0.37	0.383	0.189	0.326	0.371	0.19	0.203	0.363
M-K test value (S)	301	−19	40	315	−291	155	−348	−492	−138
Standardized value of S	0.855	−0.0513	0.111	1.132	−1.045	0.555	−1.341	−1.897	−0.53
Approximate p-value	0.196	0.48	0.456	0.129	0.148	0.289	0.09	0.0289	0.298
Number of slopes	5253	5253	5253	3828	3828	3828	3486	3486	3486
M1′	2283	2283	2283	1642	1642	1642	1489	1489	1490
One-sided 95% lower limit of slope	2970	2970	2970	2186	2186	2186	1997	1997	1996
95% LCL of Slope (0.025)	−0.0005	−0.0008	−0.0018	−0.0004	−0.0015	−0.0017	−0.0023	−0.0025	−0.0050
95% UCL of Slope (0.975)	0.0013	0.0007	0.0019	0.0016	0.0004	0.0028	0.0005	0.0000	0.0020

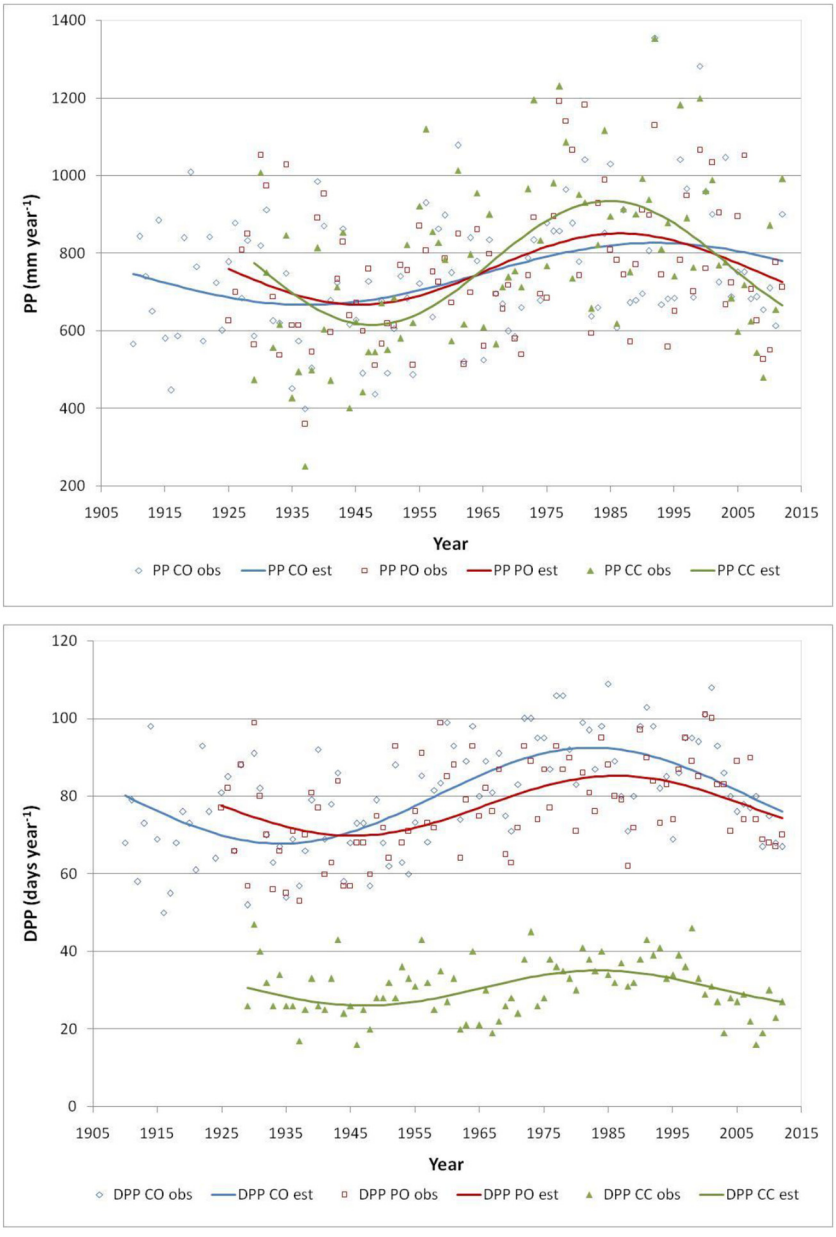

Fig. 6. Interannual variation of observed values (obs) of total rainfall (PP, above) and number of rainy days (DPP, below) in Córdoba Observatorio (CO), Pilar Observatorio (PO) and Colonia Caroya (CC), with their respective adjustments to a sine function (est). The correlation and regression coefficients of sine model are shown in Table 10.

Table 10
Regression and determination coefficients (R^2) obtained for different rainfall indicators with linear, sine and 3rddegree polynomial models at the central region of Argentina: Córdoba Observatorio (CO); Pilar Observatorio (PO) and Colonia Caroya (CC).

Weatherstation	Index	Linear			Sine				3rddegree polynomial				
		a	b	R^2	$\bar{Y}$	A	B	R^2	a	b	c	d	R^2
CO	PP	−2206	1.506	0.068	747.2	79.85	1.073	0.115	1.23E + 07	−18,813	9.584	−0.0016	0.111
PO		−1913	1.357	0.039	759.7	91.55	0.944	0.131	3.10E + 07	−47,299.61	24.048	−0.0041	0.134
CC		−5781	3.327	0.145	775.2	159.85	0.894	0.262	3.77E + 07	−57,604.65	29.363	−0.005	0.311
CO	DPP	−328.5	0.208	0.197	80.1	12.34	0.948	0.369	1.94E + 06	−2980.77	1.524	−0.0003	0.384
PO		−234.5	0.158	0.118	77.5	7.72	0.938	0.202	2.12E + 06	−3235.61	1.647	−0.0003	0.238
CC		−7.19	0.019	0.004	30.6	4.54	0.876	0.182	2.24E + 06	−3417.71	1.737	−0.0003	0.247
PO	PPmax	−310.3	0.194	0.049	72.5	11.73	0.967	0.132	3.81E + 06	−5808.01	2.952	−0.0005	0.133
CC		−818.8	0.461	0.17	88.9	18.06	0.885	0.205	2.33E + 06	−3583.5	1.835	−0.0003	0.277
CO	PPCV	−1.18	0.001	0.044	0.96	0.003	0.534	0.0002	−2097.31	3.19	−0.002	2.74E−07	0.047
PO		−1.79	0.001	0.054	0.94	0.024	0.570	0.012	−10,053.26	15.33	−0.008	1.30E−06	0.066
CC		−0.538	0.0008	0.012	1.06	−0.029	0.443	0.013	−15,734.05	23.94	−0.012	2.05E−06	0.028

In linear and polynomial models a: interception; b, c, and d: coefficient of the first, second, and third degree, respectively. In the sine model $\bar{Y}$ is the mean value, A is the amplitude and B is the coefficient of the period ($2\pi/B$).
References: PP: Total amount of rain; DPP: number of rainy days; PPmax: maximum daily value; PPCV: Coefficient of variation of PP.

full correspondence with the dynamics of change experienced by the other attributes of rainfall in this region. Thus, since the time series of PP, DPP and PPmax are all in phase, the increase (decrease) of total amounts of rainfall is explained by the increase (decrease) in both the number of events and their intensity.

In the climate change domain, the analysis of a time series on a secular scale is necessary because it allows the modality of long-term variability in a territory to be examined more exhaustively, providing information to refute or confirm the behavior of a shorter database (Villafuerte et al., 2014). It is evident that the quantity, frequency and intensity of rainfall tend to decrease in recent years in the central region of Argentina, in contrast to the sustained increase projected by the results of the linear model.

Finally, to analyze the changes in rainfall variability, Fig. 8 shows the fluctuation of the coefficient of variation of PP (PPCV) in central Argentina. As, in this case, the sine model was not suitable to represent rainfall variation, the records were also adjusted to a 3rddegree polynomial function. However, there is a greater dispersion of the data and the fluctuations are less pronounced than in the previously analyzed indicators, with lower coefficients of determination, practically similar to those of the linear model (Table 10). Although this long-term fluctuation cannot be validated in statistical terms, the variation would be opposite to PP, DPP and PPmax, so that the variability of rain tends to increase during the driest period and to decrease during the wet phase of the cycle.

4. Conclusions

According to rainfall records from three meteorological stations, selected to guarantee reliability because of their geographical proximity, temporal extension and continuity of data, the secular evaluation of different rainfall attributes reveals a periodic behavior of rain fallin the central region of Argentina, even though the Mann-Kendall and Theil-Sen tests also validate an increasing linear trend.

Compared to Córdoba Observatory and Pilar Observatory, both weather stations of the official network, rainfall data of Colonia Caroya present an anomalous behavior with fewer rainfall days (DPP) and so, in addition to its non-homogeneous behavior, this information should be used carefully. The total amount of rainfall (PP), annually or semi-annually, presents a very similar behavior for the three stations and

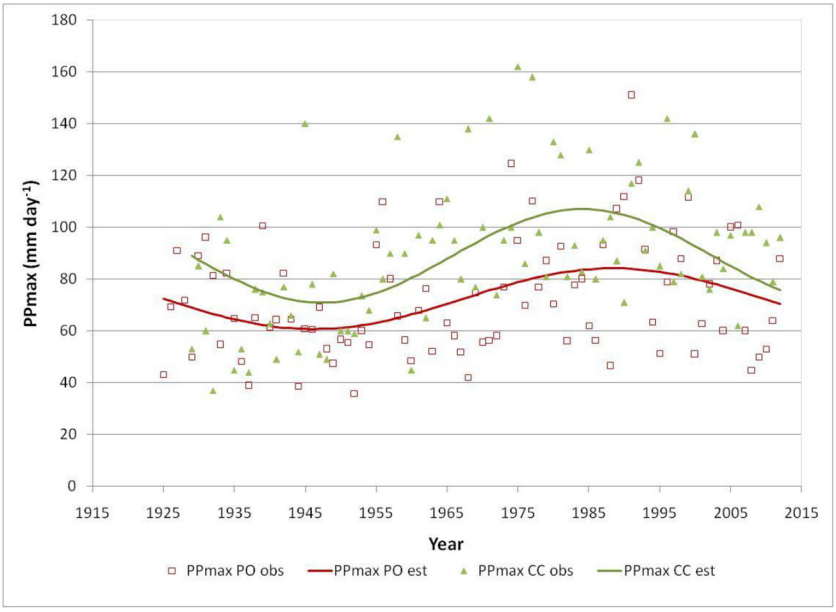

Fig. 7. Interannual variation of the observed values (obs) of maximum daily rainfall (PPmax) in Pilar Observatorio (PO) and Colonia Caroya (CC), with their respective adjustments to a sine function (est). The correlation and regression coefficients of sine model are shown in Table 10.

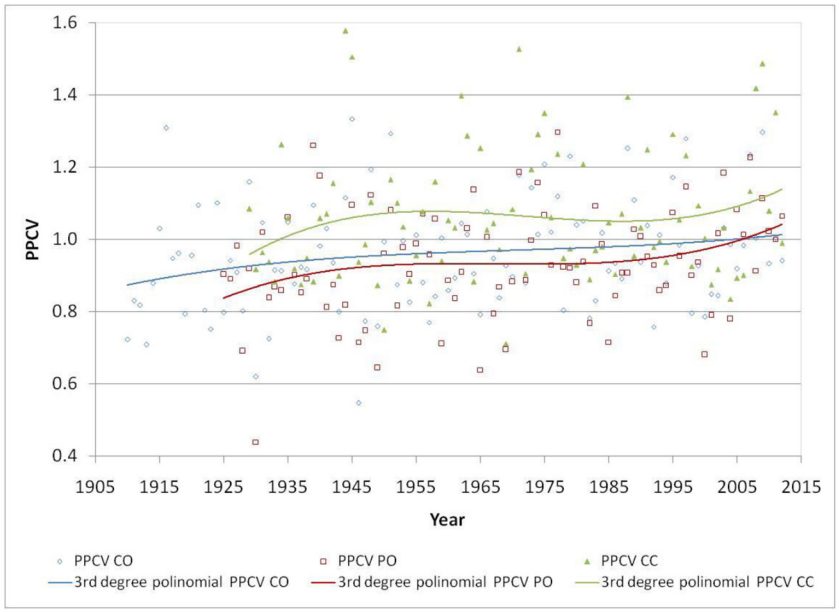

Fig. 8. Interannual variation of total rain variability (PPCV) in Córdoba Observatorio (CO), Pilar Observatorio (PO) and Colonia Caroya (CC), with their respective adjustments to a third-degree polynomial function. The correlation and regression coefficients of the polynomial model are shown in Table 10.

this, together with the homogeneity, supports the secular assessment of the rainfall regime.

The long-term variation of the rainfall amount, frequency (DPP) and intensity (PPmax), on an annual scale and during the warm semester, can be represented in periodic terms by the sine function, which exhibits a dry phase during the period between 1930 and 1950, then a wet phase that reached maximum values around the 1980s and 1990s. After this maximum, the current period suggests that values tend to decrease, in contrast to the dynamics of the constant increase of CO_2 in the atmosphere and the sustained increase of global temperature. This dissociation undermines the hypothesis of a possible intensification of the hydrological cycle in the region and, in particular, of the rainfall regime.

The temporal variations in the amount, frequency and intensity of rain have occurred in phase, so that during the dry (wet) stage not only does the number of events decrease (increase) but also the intensity of the rain, which explains the decrease (increase) of the total accumulated value.

This same periodic fluctuation also explains the growing linear trend observed in the region during the last 50 years of the 20th century, considering a shorter time series that covers only an intermediate section between a dry phase and then a wetter one. For this reason, climate change studies should use time series that are as extensive as possible, to be able to carry out more exhaustive analyses of rainfall behavior, avoid misinterpretation when shorter databases are analyzed and to permit a better understanding of climate variability.

References

Alexander, L.V., Zhang, X., Peterson, T.C., Caesar, J., Gleason, B., Klein Tank, A.M.G., Haylock, M., Collins, D., Trewin, B., Rahimzadeh, F., Tagipour, A., Ambenje, P., Rupa Kumar, K., Revadekar, J., Griffiths, G., Vincent, L., Stephenson, D.B., Burn, J., Aguilar, E., Brunet, M., Taylor, M., New, M., Zhai, P., Rusticucci, M., Vazquez-Aguirre, J.L., 2006. Global observed changes in daily climate extremes of temperature and precipitation. J. Geophys. Res. 1, 111. http://dx.doi.org/10.1029/2005JD006290.

Allan, R.P., Soden, B.J., 2008. Atmospheric warming and the amplification of precipitation extremes. Science 321, 1481–1484.

Allen, M.R., Ingram, W.J., 2002. Constraints on future changes in climate and the hydrologic cycle. Nature 418, 224–232.

Aragón, R., Jobbágy, E.G., Viglizzo, E.F., 2010. Surface and groundwater dynamics in the sedimentary plains of the Western Pampas (Argentina). Ecohydrology. http://dx.doi.org/10.1002/eco.149.

Camargo, M., Hubbard, K.G., 1999. Spatial and temporal variability of daily weather variables in sub-humid and semi-arid areas of the United States high plains. Agric. For. Meteorol. 93, 141–148.

Carreño, L., Viglizzo, E., 2011. Provisión de servicios ecológicos y gestión de los ambientes rurales en Argentina. Ediciones INTA (74 pp).

Chowdhury, R.K., Beecham, S., 2010. Australian rainfall trends and their relation to the Southern Oscillation Index. Hydrol. Process. 24, 504–514.

Cislaghi, M., De Michele, C., Ghezzi, A., Rosso, R., 2005. Statistical assessment of trends and oscillations in rainfall dynamics: analysis of long daily Italian series. Atmos. Res. 77, 188–202.

Costa, A.C., Soares, A., 2009. Trends in extreme precipitation indices derived from a daily rainfall data base for the south of Portugal. Int. J. Climatol. 29, 1956–1975.

Courtillot, V., Le Mouël, J.-L., Kossobokov, V., Gibert, D., Lopes, F., 2013. Multi-decadal trends of global surface temperature: a broken line with alternating ~30 yr linear segments? Atmos. Clim. Sci. 3, 364–371.

Dai, A., Fung, I.Y., Del Genio, A.D., 1997. Surface observed global land precipitation variations during 1900–88. J. Clim. 10, 2943–2962.

FAOCLIM 2, 2001. World-wide agroclimatic database. In: FAOCLIM CD-ROM v. 2.01.

Glave, A., 2006. Influencia climática en el sudoeste bonaerense y sudeste de La Pampa. Acaecer 31 (360), 18–23.

González, M., Barros, V., 1998. The relation between tropical convection in South America and the end of a dry period in subtropical Argentina. Int. J. Climatol. 18, 1669–1685.

Greene, A.M., Goddard, L., Cousin, R., 2011. Web tool deconstructs variability in twentieth-century climate. Eos Trans. AGU 92 (45), 397–398.

Huntington, T.G., 2011. Climate warming-induced intensification of the hydrologic cycle: an assessment of the published record and potential impacts on agriculture. Adv. Agron. 109, 1–52.

Irmak, S., Kabenge, I., Skaggs, K.E., Mutiibwa, D., 2012. Trend and magnitude of changes in climate variables and reference evapotranspiration over 116-yr period in the Platte River Basin, central Nebraska–USA. J. Hydrol. 420–421, 228–244.

Jones, J.R., Schwartz, J.S., Ellis, K.N., Hathaway, J.M., Jawdy, C.M., 2015. Temporal variability of precipitation in the Upper Tennessee Valley. J. Hydrol. 3, 125–138.

Kenyon, J., Hegerl, G., 2010. Influence of modes of climate variability on global precipitation extremes. J. Clim. 23, 6248–6262.

Killam, D., Bui, A., Ladochy, S., Ramirez, P., Willis, J., Patzert, W., 2014. California getting wetter to the North, drier to the South: natural variability or climate change? Climate 2, 168–180.

Klyashtorin, L.B., Borisov, V., Lyubushin, A., 2009. Cyclic changes of climate and major commercial stocks of the Barents Sea. Mar. Biol. Res. 5, 4–17.

de la Casa, A.C., Nasello, O.B., 2010. Breakpoints in annual rainfall trends over Córdoba, Argentina. Atmos. Res. 95, 419–427.

de la Casa, A.C., Nasello, O.B., 2012. Low frequency oscillation of rainfall in Córdoba, Argentina, and its relation with solar cycles and cosmic rays. Atmos. Res. 113, 140–146.

de la Casa, A.C., Nasello, O.B., 2015. Análisis periódico de las condiciones hidrológicas en la Provincia de Córdoba, Argentina. Anales AFA 26 (4), 170–176.

de la Casa, A.C., Ovando, G.G., 2014. Climate change and its impact on agricultural potential in the central region of Argentina between 1941 and 2010. Agric. For. Meteorol. 195–196, 1–11.

de la Casa, A.C., Ovando, G.G., Rodríguez, A.R., 2004. Criterios basados en la probabilidad de la precipitación para evaluar el riesgo agroclimático del cultivo de trigo de

secano en la provincia de Córdoba, Argentina. Rev. Bras. Agrometeorol. 12 (2), 333–339.
Lázaro, R., Rodrigo, F.S., Gutiérrez, L., Domingo, F., Puigdefábregas, J., 2001. Analysis of a 30-year rainfall record (1967–1997) in semi-arid SE Spain for implications on vegetation. J. Arid Environ. 48, 373–395.
Liang, L., Li, L., Liuet, Q., 2011. Precipitation variability in Northeast China from 1961 to 2008. J. Hydrol. 404, 67–76.
Limsakul, A., Singhruck, P., 2016. Long-term trends and variability of total and extreme precipitation in Thailand. Atmos. Res. 169, 301–317.
Lucero, O.A., Rozas, D., 2002. Characteristics of aggregation of daily rainfall in a middle-latitudes region during a climate variability in annual rainfall amount. Atmos. Res. 61, 35–48.
Lyubushin, A.A., Klyashtorin, L.B., 2012. Short term global Dt prediction using (60–70)-years periodicity. Energy Environ. 23, 75–85.
Machado, E.A.M., Marchetti, A.A., 1955. Régimen de días de lluvia en la República Argentina. Meteor-Forschung 4, 243–276.
Mantua, N.J., Hare, S.R., 2002. The pacific decadal oscillation. J. Oceanogr. 58, 35–44.
Nasri, M., Modarres, R., 2009. Dry spell trend analysis of Isfahan Province. Iran. Int. J. Climatol. 29, 1430–1438.
Ohlson, J.A., Seil, K., 2014. Linear Valuation Without OLS: the Theil-Sen Estimation Approach, Available at SSRN: https://ssrn.com/abstract=2276927 or, https://doi.org/10.2139/ssrn.2276927
Peel, M.C., Finlayson, B.L., Mcmahon, T.A., 2007. Updated world map of the Köppen-Geiger climate classification. Hydrol. Earth Syst. Sci. 11, 1633–1644.
Pérez, S., Sierra, E., Casagrande, G., Vergara, G., Berna, F., 2003. Comportamiento de las precipitaciones (1918/2000) en el centro oeste de la provincia de Buenos Aires (Argentina). Rev. Fac. Agronomía - UNLPam 14 (1/2), 39–46.
Porto De Carvalho, J.R., Delgado Assad, E., Fortes De Oliveira, A., Silveira Pinto, H., 2014. Annual maximum daily rainfall trends in the midwest, southeast and southern Brazil in the last 71 years. Weather Clim. Extrem. 5-6, 7–15.
Rashid, M.M., Beecham, S., Chowdhury, R.K., 2014. Influence of climate drivers on variability and trends in seasonal rainfall in the Onkaparinga catchment in South Australia: A wavelet approach. 13th International conference on Urban Drainage (ICUD) 2014, 7–12 September, Kuching, Sarawak, Malaysia, Kuching, Sarawak, Malaysia.
Rashid, M.M., Beecham, S., Chowdhury, R.K., 2015a. Assessment of trends in point rainfall using continuous wavelet transforms. Adv. Water Resour. 82, 1–15.
Rashid, M.M., Beecham, S., Chowdhury, R.K., 2015b. Statistical characteristics of rainfall in the Onkaparinga catchment in South Australia. J. Water Clim. Change 6 (2), 352–373.
Rashid, M.M., Beecham, S., Chowdhury, R.K., 2016. Simulation of extreme rainfall and projection of future changes using the GLIMCLIM model. Theor. Appl. Climatol. 1–14.
Ravelo, A.C., Irastorza, R.O., Zanvettor, R.E., 2003. Zonificación de la región Pampeana Argentina según tendencias de series pluviométricas (1931–2000). Rev. Argent. Agrometeorol. 3-4, 85–90.
Roberto, Z.E., Casagrande, G., Viglizzo, E.F., 1994. Lluvias en la Pampa central: tendencias y variaciones del siglo. Cambio Climático y Agricultura en la Región Pampeana, Bol. INTA La Pampa-San Luis N°2. (25 pp).
Scafetta, N., 2010. Empirical evidence for a celestial origin of the climate oscillations and its implications. J. Atmos. Sol. Terr. Phys. 72, 951–970.
Sen, P.K., 1968. Estimates of the regression coefficient based on Kendall's tau. J. Am. Stat. Assoc. 63 (324), 1379–1389.
Sneyers, R., 1990. On the statistical analysis of series of observations. In: Tech. Note 143, WMO-N° 415, (192 pp).
Sneyers, R., 1997. Climate chaotic instability: statistical determination and theoretical background. Environmetrics 8, 517–532.
Soltani, M., Rousta, I., Modir Taheri, S., 2013. Using Mann-Kendall and time series techniques for statistical analysis of long-term precipitation in Gorgan Weather Station. World Appl. Sci. J. 28 (7), 902–908.
Theil, H., 1950. A rank-invariant method of linear and polynomial regression analysis. Nederland. Akadem. Wetenchap. Ser. A 53, 386–392.
Todisco, F., Vergni, L., 2008. Climatic changes in Central Italy and their potential effects on corn water consumption. Agric. For. Meteorol. 148, 1–11.
Tomé, A.R., Miranda, P.M.A., 2004. Piecewise linear fitting and trend changing points of climate parameters. Geophys. Res. Lett. 31, L02207. http://dx.doi.org/10.1029/2003GL019100.
Trenberth, K.E., Dai, A., Rasmussen, R.M., Parsons, D.B., 2003. The changing character of precipitation. Bull. Am. Meteorol. Soc. 84, 205–217.
Trenberth, K.E., Jones, P.D., Ambenje, P., Bojariu, R., Easterling, D., Tank, A.K., Parker, D., Rahimzadeh, F., Renwick, J.A., Rusticucci, M., Soden, B., Zhai, P., 2007. Observations: surface and atmospheric climate change. In: Solomon, S., Qin, D., Manning, M., Chen, Z., Marquis, M., Averyt, K.B., Tignor, M., Miller, H.L. (Eds.), Climate Change 2007: The Physical Science Basis. Contribution of Working Group I to the Fourth Assessment Report of the Intergovernmental Panel on Climate Change. Cambridge University Press, Cambridge, UK and New York, NY, pp. 235–336.
U.S. Environmental Protection Agency (EPA), 2016. ProUCL 5.1.00 Statistical Software for Environmental Applications for Datasets with and without Nondetect Observations. Office of Research and Development. http://www.epa.gov/esd/tsc/TSC_form.htm.
Viglizzo, E.F., 2010. El agro, el clima y el agua en La Pampa Semiárida: Revisando paradigmas. Anales de Agronomía y Veterinaria (ANAV), Tomo LXIV, 251-267.
Viglizzo, E.F., Roberto, Z.E., Filippín, M.C., Pordomingo, A.J., 1995. Climate variability and agroecological change in the central pampas of Argentina. Agric. Ecosyst. Environ. 55, 7–16.
Villafuerte, M.Q., Matsumoto, J., Akasaka, I., Takahashi, H.G., Kubota, H., Cinco, T.A., 2014. Long-term trends and variability of rainfall extremes in the Philippines. Atmos. Res. 137, 1–13.
Willems, P., Olsson, J., Arnbjerg-Nielsen, K., Beecham, S., Pathirana, A., Gregersen, I.B., Madsen, H., Nguyen, V.-T.-V., 2012. Impacts of Climate Change on Rainfall Extremes and Urban Drainage Systems. IWA Publishing, London, UK, pp. 238.
Zhao, J., Huang, Q., Chang, J., Liu, D., Huang, S., Shi, X., 2015. Analysis of temporal and spatial trends of hydro-climatic variables in the Wei River basin. Environ. Res. 139, 55–64.